Applied Surface Science 36 (1989) 460–470
North-Holland, Amsterdam

THE STRUCTURE OF NANOCRYSTALLINE SILICON FORMED BY LASER-INDUCED EXPLOSIVE CRYSTALLIZATION

W.C. SINKE *, T. WARABISAKO, M. MIYAO, T. TOKUYAMA **

Central Research Laboratory, Hitachi Ltd., P.O. Box 2, Kokubunji, Tokyo 185, Japan

and

S. ROORDA

FOM-Institute for Atomic- and Molecular Physics, Kruislaan 407, 1098 SJ Amsterdam, The Netherlands

Received 2 June 1988; accepted for publication 24 June 1988

The structure of nanocrystalline silicon formed by pulsed laser induced explosive crystallization of amorphous silicon has been studied using Raman spectroscopy. It is found that the properties of nanocrystalline silicon are independent of the laser energy density used to initiate explosive crystallization. From the spectrum in the low-wavenumber region it is inferred that the grains in nanocrystalline silicon are highly distorted. The average grain size, as determined from the position of the main peak in the spectrum, is 5–7 nm. Annealing at 500–600 °C results in a decrease of the distortion and an increase in average grain size by 1–2 nm.

1. Introduction

Nanocrystalline silicon (nc-Si), also referred to as as fine-grained polycrystalline silicon (fgp-Si) or microcrystalline silicon (μc-Si), forms the subject of many recent studies [1–19]. The term "nanocrystalline" is used for materials with an average grain size of several nanometers to several tens of nanometers. As a result of the limited grain size, the material properties of nc-Si differ substantially from those of monocrystalline silicon (c-Si) and large-grained polycrystalline silicon (lgp-Si). Also, as a result of the crystalline order in the grains, the properties clearly differ from those of amorphous silicon (a-Si). For these reasons nc-Si is an interesting class of materials both from the funda-

* Present address: FOM-Institute for Atomic- and Molecular Physics, Kruislaan 407, 1098 SJ Amsterdam, The Netherlands.

** Present address: Institute of Applied Physics, University of Tsukuba. Sakura-mura, Ibaraki-ken 305, Japan.

0169-4332/89/$03.50 © Elsevier Science Publishers B.V.
(North-Holland Physics Publishing Division)

mental point of view and for applications. Similar to a-Si, nc-Si can be prepared in a pure and in a hydrogenated form (nc-Si : H) [7,14,16]. In nc-Si : H, grain boundaries are passivated by hydrogen, which enables application in photovoltaic and other thin-film devices.

Until now, mainly nc-Si formed by chemical vapour deposition (thermal- [17], plasma- [5,9,13,14,16] or photo- [11]), chemical transport [1,2,4,7,8,19], evaporation [10] and random crystallization of a-Si [12,15] has been studied. These preparation methods have in common that they involve only gas- or solid-phase reactions.

Recently, a new way to form nc-Si has been investigated, namely explosive crystallization (EC) [20] of a-Si, induced by pulsed-laser irradiation [18,21–32] or scanning continuous-wave laser irradiation [33]. This method involves ultra-rapid solidification of highly undercooled liquid silicon (l-Si) and therefore it differs from all methods employed until now. Although there are still fundamental questions concerning triggering and propagation of EC [34], a variety of experiments has yielded a rather consistent phenomenological picture of the melting and solidification processes involved. This is illustrated in fig. 1, which shows schematic cross-sections at different times of an a-Si

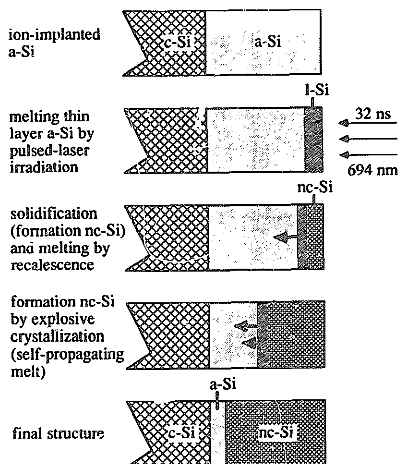

Fig. 1. Schematic of nc-Si formation by laser-induced explosive crystallization of a-Si.

sample during EC, induced by pulsed-laser irradiation at an energy density just above the threshold for surface melting. nc-Si is formed by solidification of a self-propagating melt, which moves inward at a velocity of 10–15 m/s [26,27,31]. The driving force for this process is the difference in free energy between a-Si and nc-Si, which results in a release of heat when a-Si is melted and subsequently crystallized.

In this paper results are presented from Raman scattering experiments on nc-Si formed by pulsed-laser induced EC of ion-implanted a-Si. Raman spectroscopy has been shown to be a very useful technique to probe structural properties of fine-grained materials [7], because it is especially sensitive to deviations from bulk-crystal properties which occur with decreasing grain size.

2. Experimental

A layer of a-Si was formed by dual P^+ implantation into Si(100). The energies and doses were 50 keV/1×10^{16} cm^{-2} and 170 keV/2×10^{16} cm^{-2}, respectively. The thickness of the resulting a-Si layer, as determined by cross-sectional transmission electron microscopy (X-TEM), was 370 nm. Pulsed-laser irradiation was performed using a homogenized *Q*-switched ruby laser (pulselength 32 ns, wavelength 694 nm) in the energy density range of 0.1 to 0.2 J cm^{-2}. The relative accuracy between different spots of the energy densities was better than 5%.

Raman spectra were measured in a backscattering geometry using a Cary 82 triple-grating monochromator with photon-counting system. The 531 nm line of a Kr laser was used as a light source. The diameter of the beam on the sample surface was ~ 0.1 mm and the total power < 150 mW. Spectra were taken with a resolution of 1 to 5 cm^{-1}, depending on the purpose of the measurement.

3. Results and discussion

3.1. Amorphous silicon and monocrystalline silicon

Fig. 2 shows a comparison between the spectrum of c-Si and a typical spectrum of a-Si. At the bottom of the figure the assignment of the various peaks is indicated (see ref. [35] for a general introduction to Raman scattering in solids). The a-Si spectrum shows four features (TA = transverse acoustic, LA = longitudinal acoustic, LO = longitudinal optic and TO = transverse optic), corresponding to different vibrational modes in the a-Si random network. The overall shape of the spectrum resembles a broadened version of the vibrational density-of-states (DOS) [36], which is due to the absence of

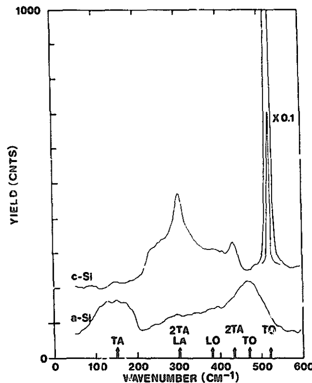

Fig. 2. Raman spectra of a-Si and c-Si. Indicated are the assignments of the various peaks (lower row refers to a-Si, upper row to c-Si). The c-Si spectrum is shifted along the vertical axis for clarity.

selection rules in a disordered solid. In c-Si, the situation is different: selection rules allow only one first-order transition (a TO phonon at ~ 521 cm^{-1}, originating from the Γ-edge of the Brillouin zone). The other features in the spectrum correspond to second-order transitions (2TA). In comparison to that of a-Si, the spectrum of c-Si has two important characteristics: the very strong TO(Γ) peak at ~ 521 cm^{-1} and the absence of any structure below 200 cm^{-1}.

3.2. Nanocrystalline silicon

The spectrum of nc-Si is expected to show features of both c-Si and a-Si, because of the crystalline yet imperfect nature of such material. More specifically, the spectral region below 200 cm^{-1} can be used as a probe for the degree of disorder [10], while the TO(Γ) peak contains information about the crystallinity [2].

Fig. 3 shows a set of Raman spectra of a-Si before and after pulsed-laser irradiation at energy densities between 0.1 and 0.2 J cm^{-2}, in comparison to the spectrum of c-Si. After irradiation at 0.101 J cm^{-2} the spectrum shows several changes when compared to that of as-implanted a-Si. The ratio of the peak intensities of the TO and TA peaks (see fig. 2) is found to increase upon irradiation. In addition, the TO peak shifts towards higher wavenumbers while

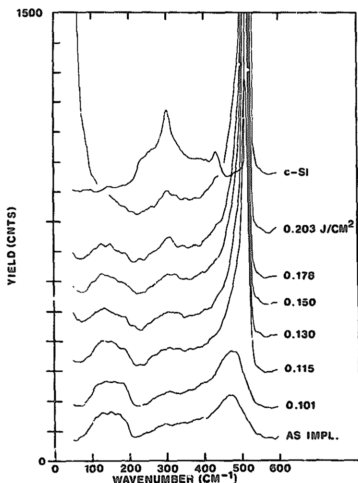

Fig. 3. Raman spectra of a-Si before and after pulsed-laser irradiation at various energy densities to induce explosive crystallization, in comparison to the spectrum of c-Si. Spectra are shifted along the vertical axis for clarity.

its width decreases. All these features are indicative of structural relaxation of a-Si, a process discussed in detail in refs. [37,38]. As the spectrum does not show any indication for crystallization, apparently the laser energy density was not sufficient to induce surface melting and EC.

After irradiation at 0.115 J cm^{-2} the spectrum shows a clear peak located around 514 cm^{-1}, which indicates the presence of crystalline silicon. The observation of a TO(Γ) peak shows that the laser energy density has now passed the threshold for surface melting and EC. The shift of this TO(Γ) with respect to that in c-Si (521 cm^{-1}) will be discussed in detail with fig. 4. Besides the TO(Γ) peak, the most interesting part of the spectrum is the region below 200 cm^{-1}. After irradiation at 0.115 J cm^{-2} and the formation of ~ 200 nm of nc-Si, as determined by X-TEM, the spectrum still shows a strong TA-like peak around 150 cm^{-1}. In comparison to the corresponding peak in a-Si, it has a different shape. The shape of the TA peak has been related to the topology of the (a-Si) network, in other words, to the distribution of 5-, 6- and 7-membered rings of atoms [39]. Therefore, although the TA peak indicates

disorder in both cases [10], the type of disorder is different for a-Si and nc-Si. This is attributed to the fact that in a distorted crystal most atoms are still expected to be in 6-membered rings, while in a-Si this is not the case. Finally, the spectrum shows a weak feature around 300 cm^{-1}, which corresponds to 2(TA)-phonon scattering in crystalline silicon.

Upon irradiation at 0.130 J cm^{-2}, again a strong TO(Γ) peak is observed. The TA-like peak is somewhat weakened, but has basically the same shape as that for irradiation at 0.115 J cm^{-2}. The weakening is attributed to a decreased contribution from underlying a-Si as the thickness of nc-Si increases with energy density. Note that the probe depth for Kr laser light of 531 nm appears to exceed the thickness of nc-Si. Irradiation at 0.150 or 0.178 J cm^{-2} does not produce significant changes in the low-wavenumber region in comparison to 0.130 J cm^{-2}. According to X-TEM, the thickness of nc-Si saturates at ~ 330 nm in these cases.

Finally, after irradiation at 0.203 J cm^{-2} the spectrum shows a strong increase in low-wavenumber scattering. This is attributed to elastic scattering and related to surface roughness, as was confirmed by scanning electron microscopy. Roughening of the surface coincides with the formation of lgp-Si on top of nc-Si (for a discussion of lgp-Si formation see, for instance, ref. [23]).

Except for relatively small changes, the Raman spectrum is remarkably constant over the whole energy density range studied. This is explained by the fact that EC is a self-sustaining process. Once initiated it is mainly governed by material properties. Thus the properties of the material formed are rather insensitive to the ignition parameter (i.e. the laser energy density).

Fig. 4 shows the TO(Γ) peaks which were out of scale in fig. 3. For reference, the peak of c-Si as well as the scattering level of a-Si are also shown.

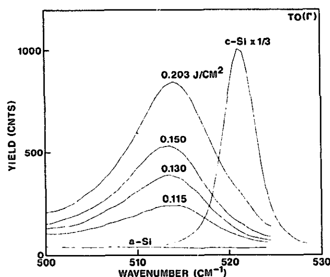

Fig. 4. TO(Γ) peaks of nc-Si formed by pulsed-laser irradiation of a-Si at various energy densities, in comparison to the peak of c-Si and the background level of a-Si.

Apart from differences in peak intensities, the figure shows that for all laser energy densities the TO(Γ) peak of nc-Si is shifted by 7–7.5 cm^{-1} in comparison to that of c-Si (521 cm^{-1} in our experiments). This shift may have several reasons. First, it can be due to thermal stress in the material, which influences the phonon "spring constant" [40]. Second, it can be due to heavy P-doping. In that case the phonon frequency is altered by electron–phonon interactions [41,42]. Third, it can be due to a very small grain size. In c-Si, selection rules only allow a TO phonon at wavevector $k \equiv 2\pi/\lambda \approx 0$. In nc-Si, the maximum wavelength which has physical meaning is approximately equal to twice the average grain size a. In such material the $k \approx 0$ selection rule is modified to $k \approx 2\pi/2a = \pi/a$ [2]. From phonon dispersion curves [43] it is then easily understood that the phonon frequency decreases with decreasing grain size.

The thermal stress observed upon pulsed-laser melting of a-Si at higher energy densities (resulting in c-Si or lgp-Si) does not exceed a value corresponding to a shift of 1–1.5 cm^{-1} [41,44,45]. This may be considered also to give an upper limit for the thermal stress upon EC. The influence of heavy P-doping on the TO(Γ) peak position was evaluated by measuring this position for P-implanted samples identical to those used to prepare nc-Si, after thermal annealing in a N_2 ambient at temperatures ranging from 600 to 1100 °C. This treatment results in single-crystallization of the a-Si layer and (partial) dopant activation. All shifts observed were less than 1 cm^{-1}. Assuming full activation, the carrier concentration in the present samples is $< 10^{21}$ cm^{-3}. According to ref. [41], this corresponds to a maximum shift of ~ 3 cm^{-1}. In fine-grained material, however, full dopant activation is not expected and the shift should be smaller than this value.

Taking into account the influence of thermal stress (1–1.5 cm^{-1}) and heavy P-doping (0.5–3 cm^{-1}) on the TO(Γ) peak position, the grain-size related shift is estimated to be between 3 and 6 cm^{-1}. According to ref. [2], this corresponds to an average grain size of 5–7 nm. These numbers are smaller than those estimated using TEM ($\sim$ 10 nm [23]), which may be due to neglect of very small grains in the latter estimate. It is noted that the critical size of grains appears to be $\sim$ 3 nm [3]. Below this value nc-Si becomes unstable with respect to the amorphous phase. Hence, the average grain size in material formed by EC is rather close to this critical value, which must result in considerable lattice strain [3]. Because of the large grain-boundary-to-volume ratio for material with an average grain size 5–7 nm, surface modes are expected to play an important role in the Raman spectrum. This gives rise to amorphous-like features [2], as observed.

Finally, fig. 4 shows that the TO(Γ) peak for nc-Si is broadened in comparison to the corresponding peak in c-Si. This is attributed to a short phonon lifetime in nc-Si [2] and to a random distribution of grain sizes.

3.3. Annealing

Fig. 5 shows the Raman spectrum of nc-Si formed by EC at 0.150 J cm^{-2}, in comparison to spectra of the same material after thermal annealing at 500 °C for 2 min and 600 °C for 10 min, respectively. The spectra of a-Si and c-Si are given for comparison.

Annealing at 500 °C results in minor changes in the regime below 500 cm^{-1}, but a clear upward shift of the TO(Γ) peak by ~ 2 cm^{-1} (see inset fig. 5). This shift is attributed to an increase of the average grain size by ~ 1 nm, probably because very small metastable grains are consumed by larger grains. Annealing for 2 min at 500 °C is sufficient to induce epitaxial regrowth of a-Si over several nanometers [46] and hence, to remove possible traces of a-Si from the nc-Si. As the spectrum below ~ 500 cm^{-1} does not show any significant changes upon annealing, it is concluded that indeed this part of the spectrum reflects the properties of nc-Si and that as-formed nc-Si does not contain considerable amounts of a-Si.

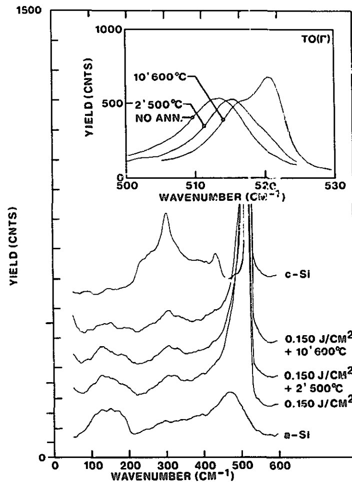

Fig. 5. Raman spectra of nc-Si formed by pulsed-laser irradiation at 0.150 J cm^{-2} before and after thermal annealing, in comparison to the spectra of a-Si and c-Si. Spectra are shifted along the vertical axis for clarity. Inset: TO(Γ) peaks of nc-Si before and after annealing on a different scale.

Annealing at 600 °C causes the TO(Γ) peak to shift upward by another 2 cm^{-1}, again corresponding to ~ 1 nm grain growth. (The peak at 521 cm^{-1} in the inset of fig. 5 is due to an enhanced contribution of the substrate and is attributed to epitaxial regrowth of the highly absorbing a-Si layer between nc-Si and c-Si and to a decrease of the absorption coefficient of nc-Si upon annealing.) In addition, the TA-like peak around 150 cm^{-1} is somewhat weakened in comparison to the other spectra, which indicates a decrease of disorder. This decrease may be related to the decreasing grain-boundary-to-volume ratio with grain growth or to the annealing of quenched-in defects. The present observation of grain growth in nc-Si at very low temperatures (in comparison to lgp-Si) is in agreement with earlier experiments on identical material [18], which have shown that nc-Si can be regrown epitaxially on c-Si at temperatures well below those required for epitaxial alignment of lgp-Si (> 1000 °C) [47]. Both grain growth and epitaxial alignment are enhanced by the large free-energy stored in grain boundaries, lattice strain and defects in nc-Si compared to lgp-Si.

4. Conclusions

The vibrational properties of nc-Si formed by EC of a-Si have been studied using Raman spectroscopy. It is found that the properties of nc-Si are independent of the laser energy density used to initiate EC. The average grain size is only 5–7 nm, as inferred from the position of the main vibrational peak. As a result of this, the grains are heavily distorted. In spite of the heavy distortion, nc-Si can be clearly distinguished from a-Si, since nc-Si consists essentially of 6-membered atomic rings, while a-Si contains both 5-, 6- and 7-membered rings. Annealing at 600 °C causes grain growth by ~ 2 nm and a reduction of the distortion.

Acknowledgements

The authors gratefully acknowledge Dr. M. Tamura for performing X-TEM This work is covered by the agreement on research collaboration between the Central Research Laboratory of Hitachi Ltd. and the FOM-Institute for Atomic- and Molecular Physics. The work at the FOM-Institute was financially supported by the Netherlands Organization for the Advancement of Research (NWO) and the Netherlands Technology Foundation (STW).

References

[1] S. Veprek, Z. Iqbal, H.R. Oswald and A.P. Webb, J. Phys. C 14 (1981) 295.
[2] Z. Iqbal and S. Veprek, J. Phys. C 15 (1982) 377.

[3] S. Vepřek, Z. Iqbal and F.-A. Sarott, Phil. Mag. 45 (1982) 137.
[4] S. Vepřek, Z. Iqbal, H.R. Oswald, F.-A. Sarott, J.J. Wagner and A.P. Webb, Solid State Commun. 39 (1981) 509.
[5] Z. Iqbal, A.P. Webb and S. Vepřek, Appl. Phys. Letters 36 (1980) 163.
[6] H. Richter, Z.P. Wang and L. Ley, Solid State Commun. 39 (1981) 625.
[7] H. Richter and L. Ley, J. Appl. Phys. 52 (1981) 7281.
[8] H. Richter, Thesis, University of Stuttgart, FRG (1982).
[9] T. Kamiya, M. Kishi, A. Ushirokawa and T. Katoda, Appl. Phys. Letters 38 (1981) 377.
[10] T. Shimada, Y. Katayama, K. Nakagawa, H. Matsubara, M. Migitaki and E. Maruyama, J. Non-Cryst. Solids 59/60 (1983) 783.
[11] T. Saitoh, T. Shimada, M. Migitaki and Y. Tarui, J. Non-Cryst. Solids 59/60 (1983) 715.
[12] E. Bustarret, B. Ranchoux, H. Hamdi, A. Deneuville, S. Huant and P. Depelsenaire, Physica B 117/118 (1983) 950.
[13] W.E. Spear, G. Willeke and P.G. Lecomber, Physica B 117/118 (1983) 908.
[14] T. Hamasaki, M. Ueda, Y. Osaka and M. Hirose, J. Non-Cryst. Solids 59/60 (1983) 811.
[15] T. Okada, T. Iwaki, H Kasahara and K. Yamamoto, Japan. J. Appl. Phys. 24 (1985) 161.
[16] Y. Mishima, S. Miyazaki, M. Hirose and Y. Osaka, Phil. Mag. 46 (1982) 1.
[17] Y. Saito, N. Ito, Y. Kameshima, R. Takeda and H. Kuwano, J. Appl. Phys. 63 (1988) 1117.
[18] S. Roorda, S. Saito and W.C. Sinke, in: Fundamentals of Beam–Solid Interactions and Transient Thermal Processing, MRS Symp. Proc. 100, Eds. M.J. Aziz, L.E. Rehn and B. Stritzker (MRS, Pittsburgh, PA, 1988) p. 417.
[19] S. Vepřek, F.-A. Sarott and Z. Iqbal, Phys. Rev. 36 (1987) 3344.
[20] A. Matsuda, A. Mineo, T. Kurosa and M. Kikuchi, Solid State Commun. 13 (1973) 1165.
[21] M.O. Thompson, G.J. Galvin, J.W. Mayer, P.S. Peercy, J.M. Poate, D.C. Jacobson, A.G. Cullis and N.G. Chew, Phys. Rev. Letters 52 (1984) 2360.
[22] W. Sinke and F.W. Saris, Phys. Rev. Letters 53 (1984) 2121.
[23] J. Narayan, C.W. White, O.W. Holland and M.J. Aziz, J. Appl. Phys. 56 (1984) 1821.
[24] R.F. Wood and G.A. Geist, Phys. Rev. Letters 57 (1986) 873.
[25] H.-D. Geiler, E. Glaser, G. Götz and M. Wagner, J. Appl. Phys. 59 (1986) 3091.
[26] J.J.P. Bruines, R.P.M. van Hal, H.M.J. Boots, A. Polman and F.W. Saris, Appl. Phys. Letters 49 (1986) 1160.
[27] D.H. Lowndes, G.E. Jellison, Jr., S.J. Pennycook, S.P. Withrow and D.N. Mashburn, Appl. Phys. Letters 48 (1986) 1389.
[28] J.J.P. Bruines, R.P.M. van Hal, B.H. Koek, M.P.A. Viegers and H.J.M. Boots, Appl. Phys. Letters 50 (1987) 507.
[29] J.J.P. Bruines, R.P.M. van Hal, B.H. Koek, M.P.A. Viegers and H.J.M. Boots, in: Beam–Solid Interactions and Transient Processes, MRS Symp. Proc. 74, Eds. M.O. Thompson, S.T. Picraux and J.S. Williams (MRS, Pittsburgh, PA, 1987) p. 91.
[30] K. Murakami, O. Eryu, K. Takita and K. Masuda, Phys. Rev. Letters 59 (1987) 2203.
[31] D.H. Lowndes, S.J. Pennycook, G.E. Jellison, Jr., S.P. Withrow and D.N. Mashburn, J. Mater. Res. 2 (1987) 648.
[32] P.S. Peercy, J.Y. Tsao, S.R. Stiffler and M.O. Thompson, Appl. Phys. Letters 52 (1988) 203.
[33] G. Auvert, D. Benhasel, A. Perio, G.A. Rozgonyi and V.T. Nguyen, in: Laser and Electron–Beam Interactions with Solids, MRS Symp. Proc. 4, Eds. B.R. Appleton and G.K. Celler (North-Holland, New York, 1982) p. 535.
[34] S. Roorda and W.C. Sinke, Appl. Surface Sci. 36 (1989) 588.
[35] M. Cardona, Ed., Light Scattering in Solids I, (Springer, Berlin, 1983)
[36] J.E. Smith, Jr., M.H. Brodsky, B.L. Crowder and M.I. Nathan, J. Non-Cryst. Solids 8–10 (1972) 179.
[37] W.C. Sinke, T. Warabisako, M. Miyao, T. Tokuyama, S. Roorda and F.W. Saris, J. Non-Cryst. Solids 99 (1988) 308.

[38] W.C. Sinke, S. Roorda and F.W. Saris, J. Mater. Res. 3 (1988), in press.
[39] P.E. Meek, Phil. Mag. 33 (1976) 897.
[40] E. Anastassakis, A. Pinczuk, E. Burnstein, F.H. Pollak and M. Cardona, Solid State Commun. 8 (1970) 133.
[41] G. Contreras, A.K. Sood, M. Cardona and A. Compaan, Solid State Commun. 49 (1984) 303.
[42] G. Contreras, M. Cardona and A. Axmann, Solid State Commun. 53 (1985) 861.
[43] G. Dolling and R.A. Cowley, Proc. Phys. Soc. 88 (1966) 463.
[44] A.K. Shukla and K.P. Jain, Phys. Rev. B 34 (1986) 8950.
[45] J.F. Morhange, G. Kanellis and M. Balkanski, Solid State Commun. 31 (1979) 805.
[46] J.S. Williams, Nucl. Instr. Methods 209/210 (1983) 219.
[47] B.Y. Tsaur and L.S. Hung, Appl. Phys. Letters 37 (1980) 648.